

## Many-pion production in $\pi^+d$ reactions at 15 GeV/c

V. Hagopian, D. Gluch, S. Hagopian, C. P. Horne, M. Jenkins, J. E. Lannutti, P.K. Williams, and B. Wind  
*Florida State University, Tallahassee, Florida 32306*

H. O. Cohn

*Oak Ridge National Laboratory, Oak Ridge, Tennessee 37830*

W. M. Bugg, G. T. Condo, T. Handler, and E. L. Hart

*University of Tennessee, Knoxville, Tennessee 37916*

(Received 3 April 1979)

The average number of charged pions produced in  $\pi^+d$  reactions at 15-GeV/c  $\pi^+$  momentum is  $3.6 \pm 0.1$  and the average number of  $\pi^0$ 's is  $1.9 \pm 0.2$ . The average number of  $\pi^0$ 's produced is essentially independent of the number of charged pions. About 45% of the events have four or more charged pions in the final state. The exclusive final states with four or more charged pions with zero or one  $\pi^0$  are presented and compared with modified phase-space background computations. Other than the well-known resonances, such as the  $\rho^0$ , no new peaks have been observed. Coherently produced multipion systems with up to seven pions are also discussed. Detailed cross-section information for every final state is presented.

### I. INTRODUCTION

This article presents new data on the six- and eight-prong events in 15-GeV/c  $\pi^+d$  interactions. Since a large percentage of the events (about 45%) has four or more charged pions in the final state, the six- and eight-prong events were studied in detail. In reality, most of the final states contain many resonances, especially  $\rho$ 's,  $\Delta$ 's and  $N^*$ 's, but the large number of final-state pions makes it almost impossible to extract the resonances from the nonresonant background. For example, each event of  $\pi^+n \rightarrow (3\pi^+)(3\pi^-)p$  has nine  $\pi^+\pi^-$  combinations; even if each event has one  $\rho^0 \rightarrow \pi^+\pi^-$ , there will be eight other  $\pi^+\pi^-$  combinations which will create a large nonresonant background. An attempt was made to fit the various mass distributions of pions to a modified phase-space calculation, where the average momentum transfer of each pion and the exponential slope of the  $t$  distribution for the nucleon was fixed at nominal values. The resulting distributions agreed amazingly well with the actual data in the nonresonant region.

In Sec. II a brief description of the experimental details is given. Section III lists the various cross sections and calculations of the average number of various particles. In this section two-, four-, six-, and eight-prong final states are presented. Section IV discusses the six-prong final states. Section V gives some results of the eight-prong final states and Sec. VI presents the coherent data for final states with up to seven pions.

### II. EXPERIMENTAL METHOD

The data come from a 890 000-picture exposure of the deuterium-filled SLAC 82-in. bubble chamber, with an rf-separated  $\pi^+$  beam at 15 GeV/c.

All the events were scanned and predigitized at Florida State University. The first 40% of the events were digitized on the University of Pennsylvania Hough-Powell device (HPD) and the rest were digitized on the University of Tennessee spiral reader at Oak Ridge National Laboratory. The pattern recognition, geometry, and kinematic computer reductions were performed at Florida State University using the ATF, POOH, TVGP, and SQUAW programs.

Four-, six-, and eight-prong events which had an identifiable stopping proton or deuteron were scanned and measured. Also measured were three-prong events with an identifiable proton of momentum less than 650 MeV/c. In addition, the strange-particle events were measured and analyzed separately. Since there were so many two-prong events, only those that had two identifiable protons were accepted and digitized. The scanning, digitizing, and programming efficiencies for the two- and four-prong events were above 90%, the six-prong events were above 75%, and the eight-prong events were about 60%. Since very few of the eight-prong events were in any exclusive final state, only the first 40% of the data were used.

Results of the four-prong events and strange-particle production events can be found in previous publications<sup>1</sup> and Ph.D. dissertations.<sup>2</sup> The total number of measured events exceeded 110 000.

### III. MULTIPLICITIES AND CROSS SECTIONS

Table I lists the various two-, four-, six-, and eight-prong final states, the corresponding number of events, the corrected partial cross sections, and the sensitivities. In each event all positive-charged tracks below 1.5-GeV/c momentum were

TABLE I. Partial cross sections, number of events, and sensitivities for nonstrange final states up to eight-prong final states.

Final state with	$\sigma$ ( $\mu\text{b}$ )	No. of events	Events/ $\mu\text{b}$
$\pi^+d \rightarrow \pi^+d$	5000 $\pm$ 1000	estimated	
$\rightarrow \pi^+np$	5000 $\pm$ 1000	estimated	
$\rightarrow p p_s X$ ( $X \equiv$ neutrals)	200 $\pm$ 25	817	4.1
$\rightarrow \pi^+ p_s X$	2000 $\pm$ 500	213	0.1
$\rightarrow \pi^+ \pi^- p p_s$	365 $\pm$ 25	3632	10.0
$\rightarrow \pi^+ \pi^- \pi^0 p p_s$	495 $\pm$ 30	4218	8.5
$\rightarrow \pi^+ \pi^- (m\pi^0) p p_s, m > 1$	1730 $\pm$ 100	12554	7.3
$\rightarrow \pi^+ \pi^+ \pi^- n p_s$	705 $\pm$ 50	3203	4.5
$\rightarrow \pi^+ \pi^+ \pi^- (m\pi^0) n p_s, m \geq 1$	4050 $\pm$ 200	18228	4.5
$\rightarrow \pi^+ \pi^+ \pi^- d$	570 $\pm$ 25	4755	8.3
$\rightarrow \pi^+ \pi^+ \pi^- \pi^0 d$	200 $^{+50}_{-100}$	2100	10.5
$\rightarrow \pi^+ \pi^+ \pi^- (m\pi^0) d, m > 1$	<100		
$\rightarrow 2\pi^+ 2\pi^- p p_s$	253 $\pm$ 17	911	3.6
$\rightarrow 2\pi^+ 2\pi^- \pi^0 p p_s$	460 $\pm$ 45	1894	4.1
$\rightarrow 2\pi^+ 2\pi^- (m\pi^0) p p_s, m > 1$	1520 $\pm$ 95	5561	3.7
$\rightarrow 3\pi^+ 2\pi^- n p_s$	320 $\pm$ 40	1393	4.4
$\rightarrow 3\pi^+ 2\pi^- (m\pi^0) n p_s, m \geq 1$	2380 $\pm$ 145	8642	3.6
$\rightarrow 3\pi^+ 2\pi^- d$	36 $\pm$ 3	252	7.0
$\rightarrow 3\pi^+ 2\pi^- (m\pi^0) d, m \geq 1$	<50		
$\rightarrow 3\pi^+ 3\pi^- p p_s$	100 $\pm$ 15	100	1.0
$\rightarrow 3\pi^+ 3\pi^- \pi^0 p p_s$	185 $\pm$ 25	217	1.2
$\rightarrow 3\pi^+ 3\pi^- (m\pi^0) p p_s, m > 1$	325 $\pm$ 40	359	1.1
$\rightarrow 4\pi^+ 3\pi^- n p_s$	160 $\pm$ 35	161	1.0
$\rightarrow 4\pi^+ 3\pi^- (m\pi^0) p p_s, m \geq 1$	1125 $\pm$ 125	1108	1.0
$\rightarrow 4\pi^+ 3\pi^- d$	2.5 $\pm$ 1.1	5	2.0

identified either by kinematics or ionization. Since the digitizing equipment measured the relative ionization for most of the tracks, less than 20% of the events were manually checked for ionization on the scanning tables. Positive tracks above 1.5 GeV/c, with the exception of final states with no missing neutrals (i.e., four constraint), were assumed to be  $\pi^+$ 's and appropriate corrections were applied to the cross sections. Very few two-prong events were measured; the partial cross sections of the  $\pi^+d$  elastic events were extrapolated from other experiments<sup>3</sup> and the remainder of the two-prong events was attributed to the breakup reaction  $\pi^+d \rightarrow \pi^+np$ .

TABLE II. Topological cross sections in mb.

$\pi^+d \rightarrow$ All 2 prong	14.6 $\pm$ 2.0
$\rightarrow$ 4 prong with $p_s$ or $d$	8.2 $\pm$ 0.4
$\rightarrow$ 4 prong other	8.1 $\pm$ 0.4
$\rightarrow$ 6 prong with $p_s$ or $d$	5.0 $\pm$ 0.3
$\rightarrow$ 6 prong other	5.0 $\pm$ 0.3
$\rightarrow$ 8 prong with $p_s$ or $d$	1.9 $\pm$ 0.2
$\rightarrow$ 8 prong other	1.8 $\pm$ 0.2
$\rightarrow$ 10 prong	1.0 $\pm$ 0.2
$\rightarrow$ Strange particles	2.9 $\pm$ 0.2
<b>Total</b>	<b>48.5</b>

The total exposure corresponds to about 20 events/ $\mu\text{b}$ . Since the scanning criteria, the selection criteria, and the efficiencies were different for various final states, the sensitivities vary from 1.0 to 10.0 events/ $\mu\text{b}$ .

Table II lists the topological cross sections for this experiment. Only  $\frac{1}{3}$  of the spectator protons ( $p_s$ ) and about  $\frac{1}{2}$  of the deuterons ( $d$ ) were observed. An estimate of the number of  $\pi^0$ 's for a particular charged final state was performed. For

TABLE III. Partial cross sections for various charged-pion configurations.  $m$  is the number of  $\pi^0$ 's and can have values of 0, 1, 2, etc. The average value of  $m$ , denoted by  $\langle m \rangle$ , is calculated for each charged final state assuming Poisson distribution. The weighted average value of  $\langle m \rangle$  is 1.93  $\pm$  0.09. The errors are statistical.

	$\sigma$ ( $\mu\text{b}$ )	$\langle m \rangle$
$\pi^+n \rightarrow \pi^+ \pi^- (m\pi^0) p$	2590 $\pm$ 105	1.65 $\pm$ 0.15
$\rightarrow 2\pi^+ 2\pi^- (m\pi^0) p$	2235 $\pm$ 105	2.00 $\pm$ 0.20
$\rightarrow 3\pi^+ 3\pi^- (m\pi^0) p$	610 $\pm$ 50	1.85 $\pm$ 0.35
$\rightarrow 2\pi^+ \pi^- (m\pi^0) n$	4755 $\pm$ 205	1.90 $\pm$ 0.15
$\rightarrow 3\pi^+ 2\pi^- (m\pi^0) n$	2700 $\pm$ 150	2.15 $\pm$ 0.30
$\rightarrow 4\pi^+ 3\pi^- (m\pi^0) n$	1285 $\pm$ 130	2.10 $\pm$ 0.50

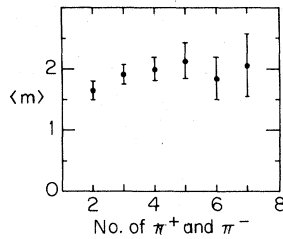


FIG. 1. Average number of  $\pi^0$ 's— $\langle m \rangle$ —as a function of the sum of  $\pi^+$  and  $\pi^-$ .

example, the cross sections for  $\pi^+n \rightarrow 2\pi^+2\pi^-(m\pi^0)p$  are known for  $m=0$ ,  $m=1$ , and  $m \geq 2$ . Even though the  $\pi^0$  multiplicity distributions are unknown, other experiments at 10 and 15 GeV/c have determined that a Poisson distribution is a fair approximation.<sup>4</sup> The data were observed to follow a Poisson distribution quite well for the three data points corresponding to  $m=0$ ,  $m=1$ , and  $m \geq 2$ . For reactions with a final-state neutron only two data points were available, corresponding to  $m=0$  and  $m \geq 1$ . Assuming that the Poisson distribution is a fair representation, the average number of  $\pi^0$ 's was calculated by fitting the data for each charged final state using a least-squares method. The results do not depend critically on the assumed  $\pi^0$  distributions. The definition  $\langle m \rangle = \sum m \sigma_m / \sigma$ , with almost any reasonable assumption for  $\sigma_m$  ( $m > 2$ ), gives similar results. For example, even if the total two-or-more  $\pi^0$  cross section is assumed to be due to  $2\pi^0$  alone, the value of  $\langle m \rangle$  drops by only 20%. A distribution of multi- $\pi^0$  cross sections that linearly decreases from its  $2\pi^0$  value to zero cross section at  $5\pi^0$  changes the final results by less than 10%.

Table III lists the reactions, total cross sections, and the computed average number of  $\pi^0$ 's. The average number of  $\pi^0$ 's for each of the six reac-

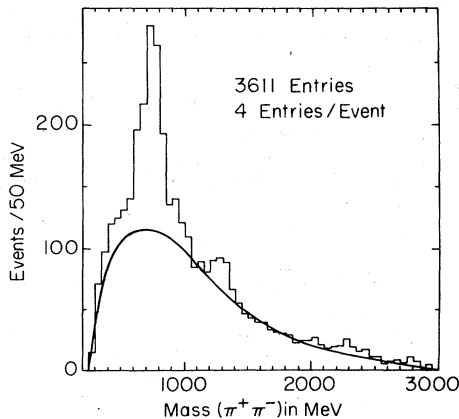


FIG. 2.  $\pi^+\pi^-$  mass distribution for the reaction  $\pi^+n \rightarrow \pi^+\pi^+\pi^-\pi^-p$ . The curve is a modified phase space normalized to events above 1400 MeV.

TABLE IV.  $\rho^0$ ,  $f$ ,  $\eta$ , and  $\omega$  cross sections for the decay modes of  $\rho^0 \rightarrow \pi^+\pi^-$ ,  $f \rightarrow \pi^+\pi^-$ ,  $\eta \rightarrow \pi^+\pi^-\pi^0$ , and  $\omega \rightarrow \pi^+\pi^-\pi^0$ .

Reaction	Cross section ( $\mu\text{b}$ )
$\pi^+n \rightarrow \rho^0\pi^+\pi^-p$	$175 \pm 20$
$\rightarrow f^0\pi^+\pi^-p$	$30 \pm 2$
$\rightarrow \rho^0f^0p$	$<3$
$\rightarrow \rho^0\rho^0p$	$20 \pm 2$
$\rightarrow \rho^0\pi^+\pi^-\pi^+\pi^-p$	$100 \pm 30$
$\rightarrow \rho^0\pi^+\pi^-\pi^0p$	$70 \pm 10$
$\rightarrow \omega\pi^+\pi^-p$	$20 \pm 2$
$\rightarrow \eta^0\pi^+\pi^-p$	$13 \pm 2$
$\pi^+d \rightarrow \rho^0\pi^+\pi^-p$	$13 \pm 2$

tions listed is about two. The calculated overall average is  $\langle m \rangle = 1.93 \pm 0.10$  and agrees well with  $\pi p$  experiments.<sup>4</sup> All the quoted errors on  $\langle m \rangle$  are statistical only. Systematic errors are expected to be less than 10%. At first our result for  $\langle m \rangle$  seemed unreasonable since charge independence (naively) implies that the number of  $\pi^0$ 's should be equal to the number of  $\pi^-$ 's. But resonances and phase-space kinematics can influence the  $\pi^0/\pi^-$  ratio. For example, an appreciable fraction of the reaction  $\pi^+n \rightarrow \pi^+\pi^-p$  proceeds via  $\rho^0$ , which has no corresponding  $\pi^0$  decays. Thus in our sample the average number of  $\pi^0$ 's for the  $\pi^+\pi^-p(m\pi^0)$  final state is lower than the overall average.

From isotopic spin considerations at very high energies for a given number of  $\pi^-$ ,  $\langle m \rangle$  should equal the number of  $\pi^-$ . At lower energies, kinematics does not allow  $\langle m \rangle$  to increase with increasing numbers of  $\pi^-$ . At very low energies, i.e., below a beam momentum of 10 GeV/c, the kinematics severely limits  $\pi^0$  production. A good discussion of this subject can be found in Ref. 5. Figure 1 is a plot of  $\langle m \rangle$  versus the number of charged pions ( $\pi^+$ 's and  $\pi^-$ 's). The distribution is essential-

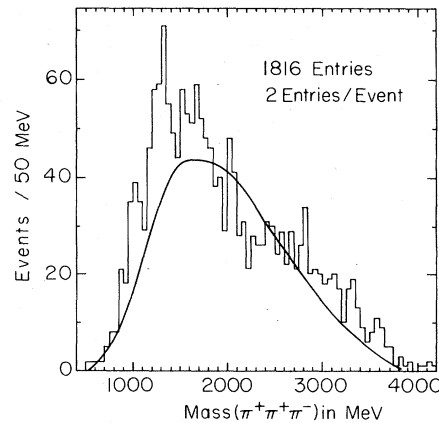


FIG. 3.  $\pi^+\pi^+\pi^-$  mass distribution for the reaction  $\pi^+n \rightarrow \pi^+\pi^+\pi^-\pi^-p$ . The curve is a modified phase space.

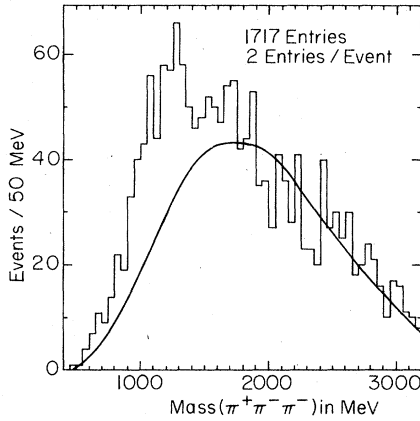


FIG. 4.  $\pi^+\pi^-\pi^-$  mass distribution for the reaction  $\pi^+n \rightarrow \pi^+\pi^+\pi^-\pi^-p$ . The curve is a modified phase space.

ly flat. At 40 GeV/c the same distribution has a small positive slope while at intersecting storage ring (ISR) energies, the slope assumes its expected value of 0.5.<sup>5</sup> Our result of a constant value of  $\langle m \rangle$ , independent of the number of charged particles, is the result of the several competing mechanisms described above. For completeness, we present the average number of charged pions for the following reactions:

$$\pi^+n \rightarrow k\pi^+ + k\pi^- + m\pi^0 + p$$

$$\langle k \rangle = 1.6 \pm 0.1, \quad \langle m \rangle = 1.8 \pm 0.2,$$

$$\pi^+n \rightarrow (k+1)\pi^+ + k\pi^- + m\pi^0 + n$$

$$\langle k \rangle = 1.4 \pm 0.1, \quad \langle m \rangle = 2.0 \pm 0.2.$$

In the latter case, the large value of  $\langle m \rangle$  compared to  $\langle k \rangle$  is probably due to having only two data points ( $m=0$  and  $m \geq 1$ ) to determine it. The error quoted is statistical. The overall average number of charged pions produced is  $3.6 \pm 0.1$ .

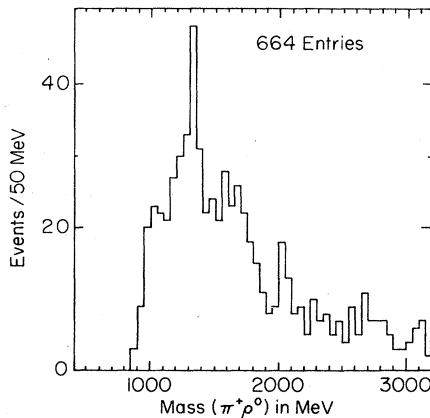


FIG. 5.  $\pi^+\rho^0$  mass distribution for the reaction  $\pi^+n \rightarrow \pi^+\pi^+\pi^-\pi^-p$ .  $\rho^0$  is defined as mass ( $\pi^+\pi^-$ ) between 680 and 830 MeV.

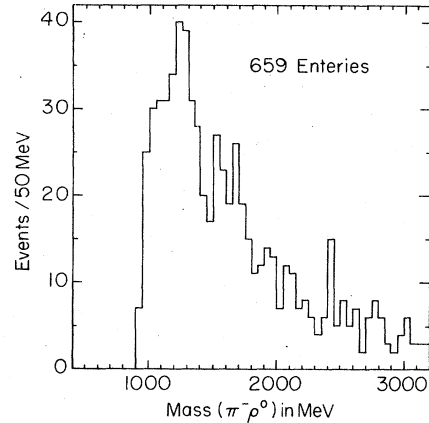


FIG. 6.  $\pi^-\rho^0$  mass distribution for the reaction  $\pi^+n \rightarrow \pi^+\pi^+\pi^-\pi^-p$ .  $\rho^0$  is defined as mass ( $\pi^+\pi^-$ ) between 680 and 830 MeV.

#### IV. SIX-PRONG FINAL STATES

Since every  $\pi^+n$  event is assumed to have a spectator proton, these events correspond to final states with four or five charged pions. The large number of pions creates a sizable combinatorial background. The common traits among the various final states are that the average transverse momentum is always about 450 MeV/c and the nucleon four-momentum-transfer distributions are all exponential. A modified phase-space calculation, using the Monte Carlo event generation program SAGE, was used where the average transverse momentum was fixed at 450 MeV/c and the  $t$  distribution fixed to agree with the experimental data. The various  $n$ -body mass distributions generated by SAGE agreed rather well with the nonresonant mass distributions of the data.

In general, the various final states show  $\rho^0$ ,  $f$ , some  $\omega$ , and some  $A_1$  or  $A_2$ . The production cross sections of these resonances decrease with the

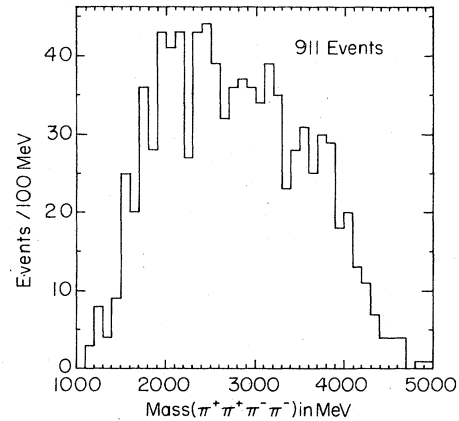


FIG. 7.  $\pi^+\pi^+\pi^-\pi^-$  mass distribution for the reaction  $\pi^+n \rightarrow \pi^+\pi^+\pi^-\pi^-p$ .

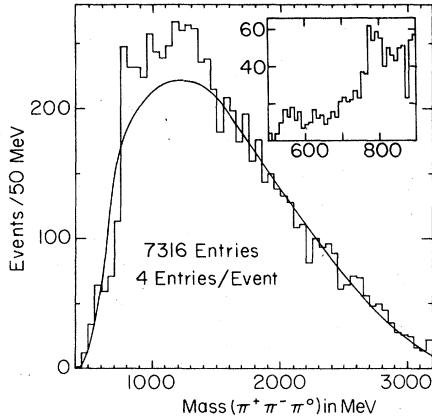


FIG. 8.  $\pi^+\pi^-\pi^0$  mass distribution for the reaction  $\pi^+n \rightarrow \pi^+\pi^+\pi^-\pi^-\pi^+p$ . The curve is modified phase space. Insert: same mass distribution in 10-MeV bins.

increasing number of final-state pions. No  $\Delta^{++}$  is observed, as anticipated, since this can be produced only by baryon exchange or via  $N^{*+} \rightarrow \Delta^{++}\pi^-$ . So  $N^*$ 's produced by charge exchange are not apparent in our data through their  $\Delta^{++}\pi^-$ -decay mode. However, small amounts of the production of  $\Delta^0$  and  $\Delta^+$  are observed.

The two final states

$$\pi^+n \rightarrow \pi^+\pi^+\pi^-\pi^-p$$

and

$$\pi^+n \rightarrow \pi^+\pi^+\pi^-\pi^0p$$

cannot be easily studied by proton targets, so these will be discussed in greater detail.

(a)  $\pi^+n \rightarrow \pi^+\pi^+\pi^-\pi^-p$ . The 911 events correspond to a cross section of  $253 \pm 17 \mu\text{b}$ . An exponential fit to the momentum transfer  $t$  of the form  $d\sigma/dt = A \exp(Bt)$  gives the values  $A = 780 \pm 70 \mu\text{b} (\text{GeV}/c)^{-2}$

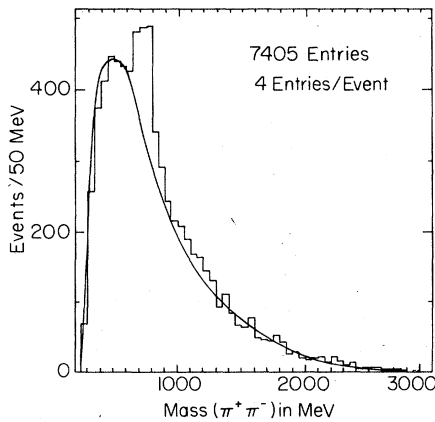


FIG. 9.  $\pi^+\pi^-$  mass distribution for the reaction  $\pi^+n \rightarrow \pi^+\pi^+\pi^-\pi^-p$ . The curve is modified phase space.

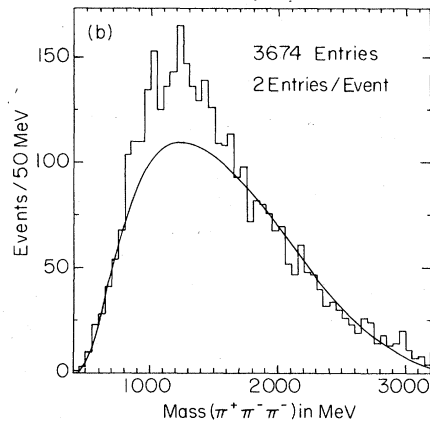
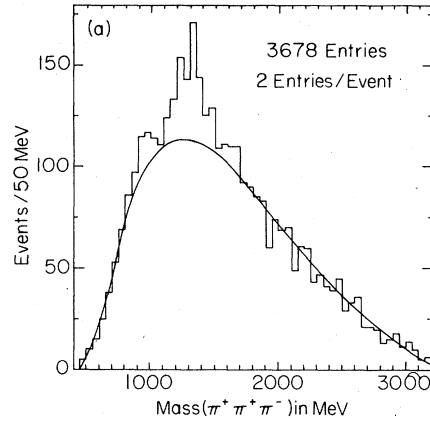


FIG. 10. Mass distributions for the reaction  $\pi^+n \rightarrow \pi^+\pi^+\pi^-\pi^-p$ : (a)  $\pi^+\pi^+\pi^-$ ; (b)  $\pi^+\pi^-\pi^-$ . The curves are modified phase space.

and  $B = 3.1 \pm 0.2 (\text{GeV}/c)^{-2}$ . A fit to the  $t' = t - t_{\min}$  distribution gives the values  $A' = 1290 \pm 100 \mu\text{b} (\text{GeV}/c)^{-2}$  and  $B' = 5.1 \pm 0.2 (\text{GeV}/c)^{-2}$ . Figure 2 shows the  $\pi^+\pi^-$  mass plot. The curve is the non-resonant calculation using the Monte Carlo generated events with a  $t$  slope of  $B = 3.1 (\text{GeV}/c)^{-2}$  and an average transverse momentum of  $\langle p_T \rangle = 450 \text{ MeV}/c$ , normalized to the nonresonant region. As can be seen, strong  $\rho^0$  and  $f^0$  signals are observed. The following resonant-production cross sections have been computed:

$$\pi^+n \rightarrow \rho^0\pi^+\pi^-p, \quad 175 \pm 20 \mu\text{b}$$

$$\pi^+n \rightarrow f^0\pi^+\pi^-p, \quad 30 \pm 2 \mu\text{b}$$

$$\pi^+n \rightarrow \rho^0\rho^0p, \quad 20 \pm 2 \mu\text{b}.$$

These and other reaction cross sections mentioned in the text are collected in Table IV. No  $\rho^0 f^0$  final state is observed and the mass plot of  $\rho^0\rho^0$  does not show notable structure. The Gottfried-Jackson decay angle in the  $\rho^0$  region shows the characteristic asymmetry of  $s$ - and  $p$ -wave interference.

Figures 3 and 4 show the  $\pi^+\pi^+\pi^-$  and  $\pi^+\pi^-\pi^-$  mass

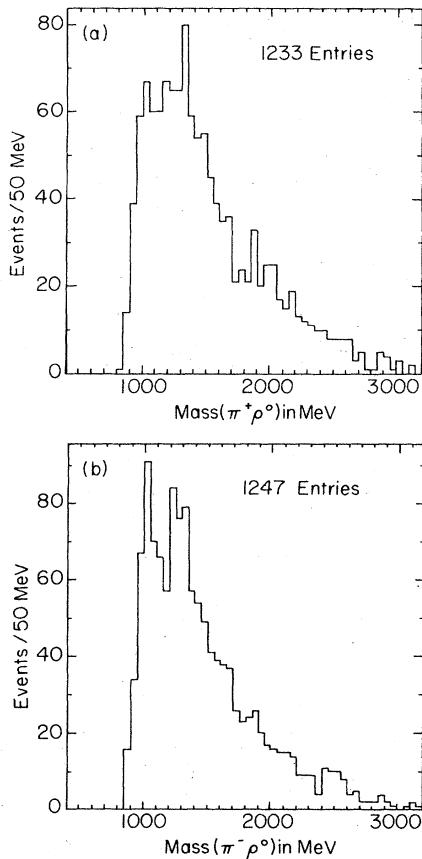


FIG. 11.  $\pi\rho^0$  mass distributions for the reaction  $\pi^+n \rightarrow \pi^+\pi^+\pi^-\pi^-\pi^0p$ . Mass of  $\rho^0$  is between 680 and 830 MeV; (a)  $\pi^+\rho^0$ , (b)  $\pi^-\rho^0$ .

plots. There is evidence of  $A_2^+$ , and perhaps some  $A_2^-$ . Figures 5 and 6 show the  $\rho^0\pi^+$  and  $\rho^0\pi^-$  mass plots, where  $\rho^0$  is defined to be a  $\pi^+\pi^-$  mass between 680 and 830 MeV. The  $A_2^+$  is very prominent

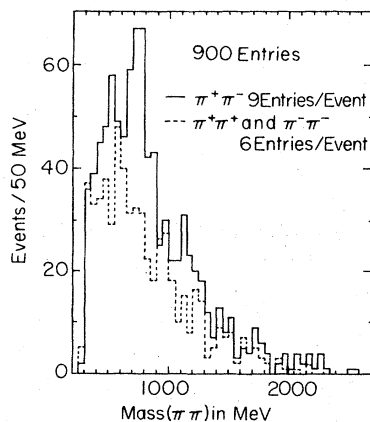


FIG. 12.  $\pi^+\pi^-$  mass distribution (solid) for the reaction  $\pi^+n \rightarrow 3\pi^+3\pi^-p$ . Dashed histogram is the sum of  $\pi^+\pi^+$  and  $\pi^-\pi^-$  mass distributions.

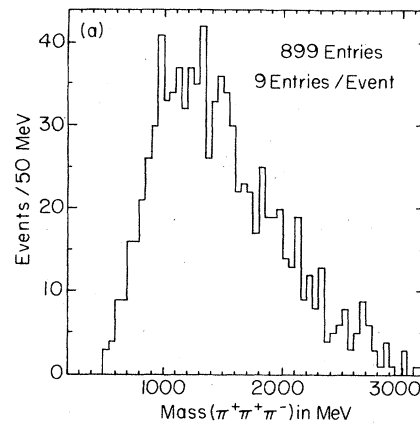


FIG. 13.  $\pi^+\pi^+\pi^+\pi^-$  mass distributions for the reaction  $\pi^+n \rightarrow 3\pi^+3\pi^-p$ .

while the  $A_2^-$  is noticeably smaller. This is expected, as  $A_2^+$  can be produced forward peripherally or even diffractively, while peripheral  $A_2^-$  requires an associated forward  $\pi^+$  and  $A_2^-$  cannot be produced diffractively at all in this reaction. Peripheral  $A_2^+$  and  $A_2^-$  may also come from  $g^0 \rightarrow A_2\pi$ . Figure 7 shows the  $4\pi$  mass plot which is essentially featureless.

(b)  $\pi^+n \rightarrow \pi^+\pi^+\pi^-\pi^-\pi^0p$ . There are 1894 events which fit this reaction; 10% are most likely multi- $\pi^0$  events. The corrected cross section for this reaction is  $460 \pm 45 \mu\text{b}$ . Even though the average number of charged pions per event is 3.6 and this reaction already has four such pions, the number of events with a single  $\pi^0$  is twice the number of events with no  $\pi^0$ s. This can be understood from a Poisson distribution with the average number of  $\pi^0$ s about two, so single- $\pi^0$  events will have a cross section about twice the size of the no- $\pi^0$  events. An exponential fit to the  $t$  and  $t'$  distributions of the nucleon yields

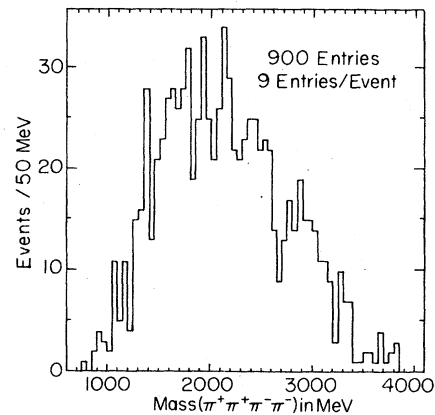


FIG. 14.  $\pi^+\pi^+\pi^-\pi^-$  mass distribution for the reaction  $\pi^+n \rightarrow 3\pi^+3\pi^-p$ .

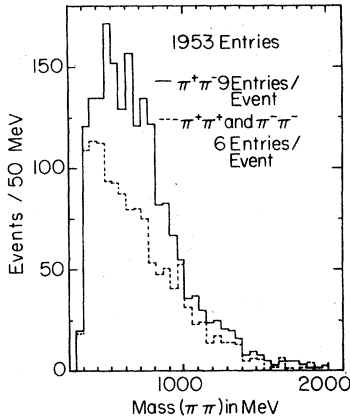


FIG. 15.  $\pi^+\pi^-$  mass distribution (solid) for the reaction  $\pi^+n \rightarrow 3\pi^+3\pi^-\pi^0p$ . Dashed histogram is the sum of  $\pi^+\pi^+$  and  $\pi^-\pi^-$  mass distributions.

$$\frac{d\sigma}{dt} = A \exp(Bt),$$

$$A = 830 \pm 160 \mu\text{b} (\text{GeV}/c)^{-2}, \quad B = 1.8 \pm 0.3 (\text{GeV}/c)^{-2}$$

$$\frac{d\sigma}{dt'} = A' \exp(B't'),$$

$$A' = 1980 \pm 200 \mu\text{b} (\text{GeV}/c)^{-2}, \quad B' = 4.3 \pm 0.1 (\text{GeV}/c)^{-2}.$$

Figure 8 shows the  $\pi^+\pi^-\pi^0$  mass plot. The insert shows the 500- to 900-MeV region in 10-MeV bins, where the  $\omega^0$  and  $\eta^0$  are visible. Resonance cross sections are given in Table IV. The curves in this and the following plots represent the modified phase-space background. Figure 9 shows the  $\pi^+\pi^-$  mass plot where the  $\rho^0$  is clearly visible, corresponding to a cross section  $70 \pm 10 \mu\text{b}$  for the reaction  $\pi^+n \rightarrow \rho^0\pi^+\pi^-\pi^0p$ . No corresponding  $\rho^-$  and  $\rho^+$  signals are observed. Figure 10 shows the  $\pi^+\pi^+\pi^-$  and  $\pi^+\pi^-\pi^-$  mass distributions. The  $\pi^+\pi^+\pi^-$  has a small, but significant, enhancement at the  $A_2$ .

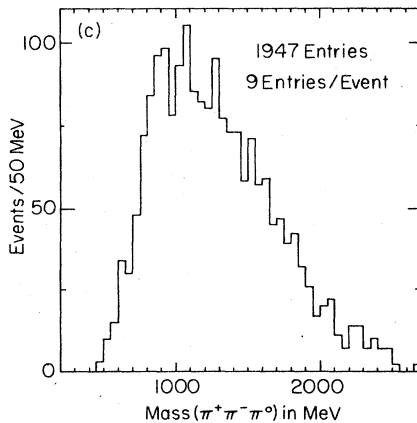


FIG. 16.  $\pi^+\pi^+\pi^-$  mass distributions for the reaction  $\pi^+n \rightarrow 3\pi^+3\pi^-\pi^0p$ .

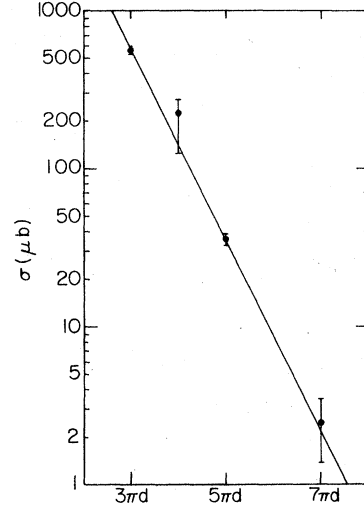


FIG. 17. Cross sections of coherent pion productions,  $\pi^+d \rightarrow (k\pi)^+d$ ;  $k=3$  is  $\pi^+\pi^+\pi^-$ ,  $k=4$  is  $\pi^+\pi^+\pi^-\pi^0$ ,  $k=5$  is  $\pi^+\pi^+\pi^+\pi^-\pi^-$ , and  $k=7$  is  $4\pi^+3\pi^-$ . Fitted line is  $\sigma (\text{mb}) = 35.9 \exp(-1.38 k)$ .

Figure 11 shows the  $\rho^0\pi^+$  and  $\rho^0\pi^-$  mass distributions. The  $A_2^+$  is not appreciably enhanced, but the  $\rho^0\pi^-$  mass plot shows two distinct peaks centered at 1020 and 1280 MeV; these peaks could correspond to the  $A_1^-$  and  $A_2^-$ , but their forward peripheral production would require an associated  $\pi^+$ , as pointed out above for the  $\pi^+n \rightarrow 2\pi^+2\pi^-p$  reaction. We do not understand why the  $(\rho\pi)^-$  mass plot shows more structure than that for  $(\rho\pi)^+$ .

## V. EIGHT-PRONG FINAL STATES

Only the first 40% of the data were scanned and measured for eight-prong events, yielding a sensitivity of about 1 event/ $\mu\text{b}$ . The combinatorial background is very large. As seen from Table I, the events  $\pi^+n \rightarrow 3\pi^+3\pi^-p$  with a single  $\pi^0$  are produced almost twice as often as events with no  $\pi^0$ , again consistent with the Poisson hypothesis that even though the number of charged pions is six, the average number of  $\pi^0$ 's is still two. Figure 12 shows the  $\pi^+\pi^-$  mass plot for the reaction  $\pi^+n \rightarrow 3\pi^+3\pi^-p$ . There may be as many as 100  $\rho^0$  events corresponding to about  $100 \pm 30 \mu\text{b}$ . The dashed histogram is the sum of  $\pi^+\pi^+$  and  $\pi^-\pi^-$  mass plots, which should be the shape of the background for  $\pi^+\pi^-$ . The  $\pi^+\pi^+\pi^-$  mass plot is shown in Fig. 13, and the  $\pi^+\pi^-\pi^-$  mass plot is very similar (not shown). The  $(4\pi)^0$  mass plot is shown in Fig. 14. With the exception of  $\rho^0 \rightarrow \pi^+\pi^-$  no other resonances are observed.

For the reaction  $\pi^+n \rightarrow 3\pi^+3\pi^-\pi^0p$ , Fig. 15 shows the  $2\pi$  mass plots, and Fig. 16 shows the  $(3\pi)$  mass plot. All these distributions are feature-

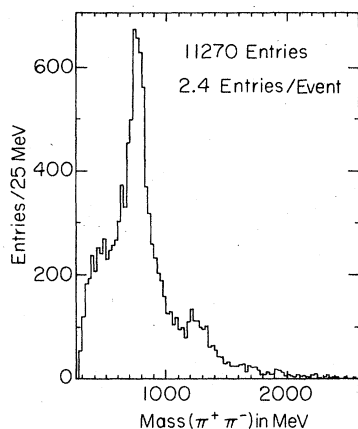


FIG. 18.  $\pi^+\pi^-$  mass distribution for the reaction  $\pi^+d \rightarrow \pi^+\pi^+\pi^-d$ . Each event is weighted by the inverse of deuteron azimuthal detection efficiency. Weight varies between 1.0 and 1.6 and average weight per event is 1.2.

less. The remaining mass plots for the eight-prong events were also examined and no resonances were observed. This is not surprising, since for every resonant two- or three-pion combinations there are ten other nonresonant combinations. In those plots where there is no combinatorial background, such as the  $6\pi$  mass distribution from the reaction  $\pi^+n \rightarrow 3\pi^+3\pi^-p$ , the data suffer from extremely limited statistics. These data cannot be appreciably improved, even if all the eight-prong events with spectators were scanned and measured. The Monte Carlo generated events reproduce the mass distributions very well.

## VI. COHERENT PION PRODUCTION

The following coherent pion production events have been observed:

Reaction	No. of events	Reaction
$\pi^+d \rightarrow \pi^+\pi^+\pi^-d$	4775	1
$\rightarrow \pi^+\pi^+\pi^-\pi^0d$	2100	2
$\rightarrow \pi^+\pi^+\pi^+\pi^-\pi^-d$	252	3
$\rightarrow \pi^+\pi^+\pi^+\pi^-\pi^-\pi^-d$	5	4

Fits were made to the  $t$  and  $t'$  of the deuteron in the form  $d\sigma/dt = A \exp(Bt)$  for the reactions 1 and 3. The slopes are as follows:

	$B$ (GeV/c) <sup>-2</sup>	$B'$ (GeV/c) <sup>-2</sup>
$\pi d \rightarrow 3\pi d$	$27.4 \pm 1.1$	$31.8 \pm 1.2$
$\pi d \rightarrow 5\pi d$	$23.0 \pm 3.5$	$30.5 \pm 3.7$

Since the exponential slopes of reactions 1 and 3

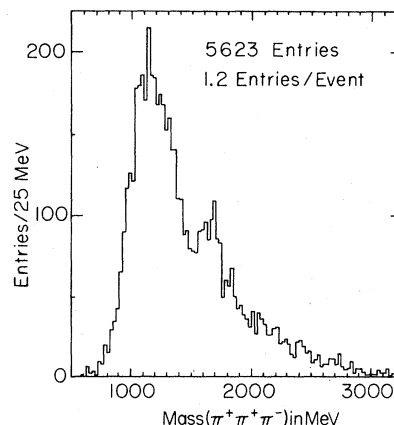


FIG. 19.  $\pi^+\pi^+\pi^-\pi^-$  mass distribution for the reaction  $\pi^+d \rightarrow \pi^+\pi^+\pi^-\pi^-d$ . Events are weighted; for explanation see Fig. 18.

are the same, the production mechanisms are most likely similar. The large values of  $B$  and  $B'$  are typical and mean that most of the production is diffractive.

Figure 17 plots the coherent cross section versus the number of pions. The distribution is an exponential of the form  $\sigma$  (mb) =  $35.9 \exp(-1.38n)$ , where  $n$  is the number of pions. It has been difficult to create a model which fits such a steeply dropping cross section. Effects due to the  $\exp(30t_{\min})$  can give perhaps a decrease by a factor of 10, but not by the needed factor of 100. An explanation of this pronounced cross-section dependence on  $n$  may involve more careful deuteron breakup considerations for the multipion final state. However, if nuclear effects are important, we would not expect  $dp \rightarrow dx$  to satisfy factorization tests compared to  $pp \rightarrow px$ , which are indeed satisfied.<sup>6</sup> Probably the rest of the decrease is accounted for by normal multiparticle statistics.

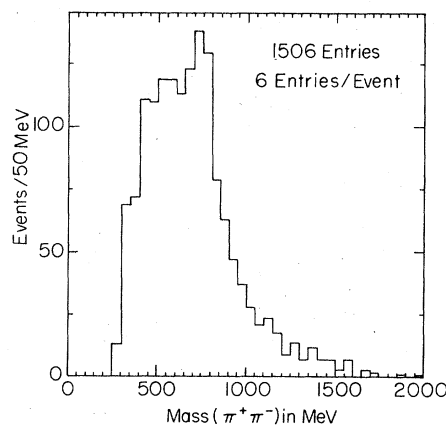


FIG. 20.  $\pi^+\pi^-$  mass distribution for the reaction  $\pi^+d \rightarrow \pi^+\pi^+\pi^+\pi^-d$ .

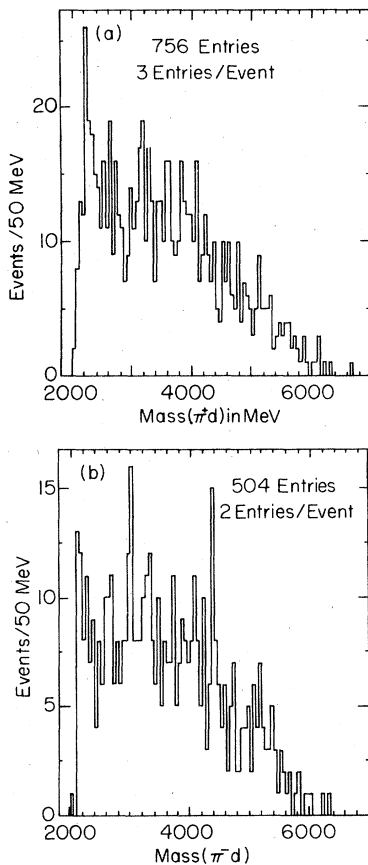


FIG. 21.  $\pi d$  mass distributions for the reaction  $\pi^+d \rightarrow \pi^+\pi^+\pi^+\pi^-\pi^-d$ : (a)  $\pi^+d$ , (b)  $\pi^-d$ .

For comparison, the ratios of cross sections for  $7\pi:5\pi:3\pi$  are 1:2.5:10 for  $\pi^+p$  interactions at 15 GeV.<sup>7</sup>

The first 40% of the data on the  $(3\pi)d$  final state were previously published.<sup>1</sup> The increase in data has not changed any of the conclusions from previous papers. For completeness, the  $2\pi$  and  $3\pi$  mass plots of reaction 1 are shown in Fig. 18 and 19; the  $\rho^0$  and  $f$  are clearly visible. In addition, the broad enhancement at the  $A_1$  is mostly  $\rho^0\pi^+$ , and similarly the  $A_3$  is also mostly  $f^0\pi^+$ .<sup>1</sup>

Reaction 3, having many more pions than reaction 1, suffers from combinatorial background. Figure 20 shows the  $\pi^+\pi^-$  mass plot; a clear  $\rho^0$  signal is observed, but no  $f^0$  is seen. The cross section for the reaction  $\pi^+d \rightarrow \rho^0\pi^+\pi^-\pi^-d$  is  $13 \pm 2 \mu\text{b}$ . Figure 21 shows the  $d\pi^+$  and  $d\pi^-$  mass plots. The  $d^{*++}(2200)$  is clearly visible, whereas only a hint of a  $d^{*0}$  is evident. The corresponding mass plots

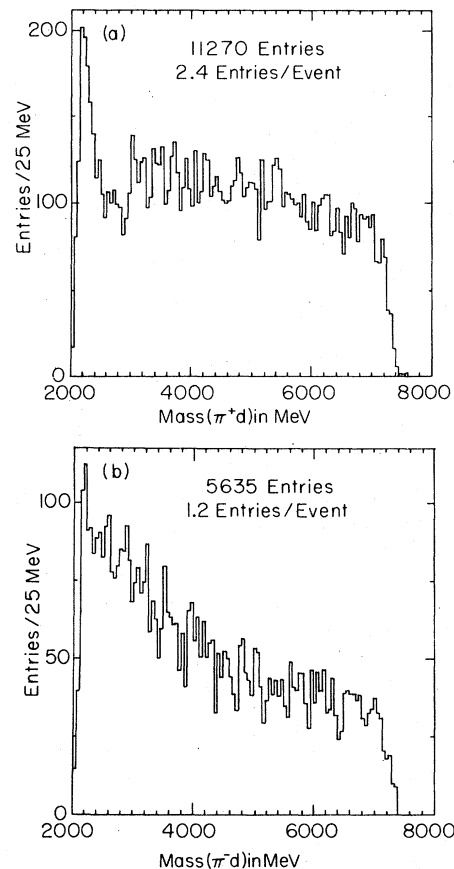


FIG. 22.  $\pi d$  mass distributions for the reaction  $\pi^+d \rightarrow \pi^+\pi^+\pi^-d$ . For event weights see Fig. 18; (a)  $\pi^+d$ , (b)  $\pi^-d$ .

for reaction 1 are shown in Fig. 22 and display similar features. The  $3\pi$ ,  $4\pi$ , and  $5\pi$  mass plots, which are not shown, are essentially featureless.

#### ACKNOWLEDGMENTS

The authors would like to thank N. D. Pewitt, J. Richey, J. Albright, J. Bensinger, and J. D. Kimel for their valuable assistance at various stages of data reduction and analysis. The efforts of the technical staff at Florida State University and the measuring staffs of the University of Pennsylvania HPD and University of Tennessee spiral reader were much appreciated. We would also like to thank the staff of the 82-in. bubble chamber at SLAC, especially R. Watt and Dr. J. Ballam. This research was supported in part by U.S. Department of Energy.

\*Present address: Lawrence Berkeley Laboratory, Berkeley, Ca.

- <sup>1</sup>C. P. Horne *et al.*, Phys. Rev. D 11, 996 (1975); J. Richey *et al.*, *ibid.* 15, 3155 (1977); C. P. Horne *et al.*, Phys. Rev. Lett. 33, 380 (1974); V. Hagopian *et al.*, *ibid.* 36, 296 (1976).
- <sup>2</sup>N. D. Pewitt, Ph.D. thesis, Florida State University (unpublished); J. Richey, Ph.D. thesis, Florida State University (unpublished); D. Wilkins, Ph.D. thesis, Florida State University (unpublished).
- <sup>3</sup>E. Bracci *et al.*, CERN/HERA Report No. 72-1, 1972

(unpublished), p. 151.

- <sup>4</sup>J. R. Elliot *et al.*, Phys. Rev. D 17, 83 (1978); Nucl. Phys. B133, 1 (1978).
- <sup>5</sup>D. Horn and F. Zachariasen, *Hadron Physics at Very High Energies* (Benjamin, Reading, Mass., 1973).
- <sup>6</sup>A. Goulianos, in *Phenomenology of Quantum Chromodynamics*, proceedings of the XIII Rencontre de Moriond, Les Arcs, France, 1978, edited by J. Trân Thanh Vân (Editions Frontières, Gif-sur-Yvette, 1978).
- <sup>7</sup>C. Baltay *et al.*, Phys. Rev. D 17, 62 (1978); see also C. N. Kennedy *et al.*, *ibid.* 17, 2888 (1978).